Journal of Solid State Chemistry 184 (2011) 2088–2096

Contents lists available at ScienceDirect

Journal of Solid State Chemistry

journal homepage: www.elsevier.com/locate/jssc

Order and disorder in $Ca_2ND_{0.90}H_{0.10}$–A structural and thermal study

Maarten C. Verbraeken [a,*], Emmanuelle Suard [b], John T.S. Irvine [a]

[a] School of Chemistry, University of St. Andrews, St. Andrews, KY16 9ST, Fife, UK
[b] Institut Laue-Langevin, BP 156, 6, rue Jules Horowitz, 38042 Grenoble Cedex 9, France

ARTICLE INFO

Article history:
Received 12 November 2010
Received in revised form
28 February 2011
Accepted 30 May 2011
Available online 14 June 2011

Keywords:
Calcium nitride hydride
Neutron powder diffraction
Thermal analysis
Order–disorder
Hydrogen storage

ABSTRACT

The structure of calcium nitride hydride and its deuterided form has been re-examined at room temperature and studied at high temperature using neutron powder diffraction and thermal analysis. When synthesised at 600 °C, a mixture of both ordered and disordered $Ca_2ND_{0.90}H_{0.10}$ phases results. The disordered phase is the minor component and has a primitive rocksalt structure (spacegroup *Fm*3*m*) with no ordering of D/N on the anion sites and the ordered phase is best described using the rhombohedral spacegroup *R*-3*m* with D and N arranged in alternate layers in (111) planes. This mixture of ordered and disordered phases exists up to 580 °C, at which the loss of deuterium yields $Ca_2ND_{0.85}$ with the disappearance of the disordered phase. In the new ordered phase there exists a similar content of vacancies on both anion sites; to achieve this balance, a little N transfers onto the *D* site, whereas there is no indication of D transferring onto the *N*-sites. These observations are thought to indicate that the D/N ordering is difficult to achieve with fully occupied anion sites. It has previously been reported that Ca_2ND has an ordered cubic cell with alternating *D* and *N* sites in the [100] directions [1]; however, for the samples studied herein, there were clearly two coexisting phases with apparent broadening/splitting of the primitive peaks but not for the ordered peaks. The rhombohedral phase was in fact metrically cubic; however, all the observed peaks were consistent with the rhombohedral unit cell with no peaks requiring the larger ordered cubic unit cell to be utilised. Furthermore this rhombohedral cell displays the same form of N–D ordering as the Sr and Ba analogues, which are metrically rhombohedral.

1. Introduction

Due to their potential to reversibly store large amounts of hydrogen, nitrogen–hydrogen compounds of the alkali and alkaline earth metals have received increasing interest over the last few years. The use of light elements is preferable in this respect, as these enable larger gravimetric storage densities. Chen et al. [2] were the first to report the viability of the Li–N–H system, which theoretically could store 10.4 wt% H_2, according to the following equations

$$Li_3N + H_2 \xrightarrow[T = 225\ ^\circ C]{pH_2 = 0.01\ bar} Li_2NH + LiH \quad (1)$$

$$Li_2NH + H_2 \xrightarrow[T = 255\ ^\circ C]{pH_2 = 0.8 bar} LiNH_2 + LiH \quad (2)$$

The first step in this absorption scheme is generally believed to have too low equilibrium pressure to be considered practically reversible. The second step, in which lithium imide is converted into lithium amide upon hydrogen absorption, still stores 6.5 wt% H_2 at reasonable temperatures and pressures, making this system a good candidate for onboard hydrogen storage purposes. Analogue hydrogen absorption reactions were studied in the Mg–N–H and Ca–N–H systems [3,4]. Ternary and quaternary systems are currently being studied to optimise absorption and desorption pressures and temperatures for typical transport applications [5–9]. A useful review of the (modified) Li–N–H system as a lightweight hydrogen storage system has been written by Gregory [10].

The Ca–N–H system has been less studied for hydrogen storage purposes, because of the relatively low gravimetric density involved in the calcium imide–amide conversion, *i.e.* 3.5 wt%. The crystal structures for the imide and amide have been reliably reported. Calcium imide has the rocksalt structure, with calcium and nitrogen coordinating each other octahedrally. Hydrogen is coordinated to nitrogen, disordered over a number of sites. Calcium amide has the tetragonal anatase structure, which is closely related to calcium imide [11,12]. It can roughly be viewed as two imide unit cells stacked on top of each other, with only half of the calcium ions now occupied. The hydrogen in the amide ions was shown to have a large degree of disorder probably due to in and out of plane movements relative to the nitrogen ion [11].

Another compound in this system, the nitride hydride (Ca_2NH), forms upon reaction of calcium nitride (Ca_3N_2) with

* Corresponding author.
E-mail addresses: mcv3@st-andrews.ac.uk (M.C. Verbraeken), jtsi@st-and.ac.uk (J.T.S. Irvine).

0022-4596/$ - see front matter © 2011 Elsevier Inc. All rights reserved.
doi:10.1016/j.jssc.2011.05.062

either calcium hydride (CaH_2) or hydrogen gas [1,13]. Compounds of the general formula M_2NX (M=Ca, Sr, Ba; X=H, F, Cl, Br) can generally be considered as M_2N, intercalated with X_2 [13]. Ordering of N and X in the crystal structure often occurs. Ca_2NH can be viewed as a slightly distorted calcium closest packed cubic structure, in which nitride and hydride ions alternately occupy the octahedral holes. The structure is therefore closely related to the rocksalt structure, but the N–H ordering in the [100] direction causes a doubling of the cubic cell [1]. A different ordering mechanism is possible, resulting in N–H ordering in the [111] direction of the cubic unit cell. This is the ordering, which is reported for $Sr_2NH(D)$ and $Ba_2NH(D)$ and involves alternating layers N and H(D) separated by layers of Ca [14,15]. These structures are rhombohedrally distorted, with slightly elongated c-values, as compared to the ideal relation, i.e. $c=2a\sqrt{6}$. These structures crystallise in the $R\bar{3}m$ spacegroup. This [111] type of N–H ordering can easily be explained by assuming that the nitride hydrides are formed from their respective subnitrides (Ae_2N, Ae=Ca, Sr and Ba) by hydrogen intercalation into the empty layers of octahedral holes between the hexagonal close-packed layers of Ca. In the subnitride, slabs of edge sharing Ae_6N octahedra are separated by layers of empty octahedral holes (Fig. 1), in which the excess electron resides [13]. It is this excess electron, which is replaced by the hydride ion in the nitride hydride.

Calcium nitride hydride apparently also absorbs hydrogen to form calcium imide [2]. The reaction is similar to reaction (1):

$$Ca_2NH+H_2 \xrightarrow{350-600\,^{\circ}C} CaNH+CaH_2 \quad (3)$$

Reaction (3) potentially stores 2.1 wt% H_2 and the reverse reaction is in fact the preferred desorption step, rather than a conversion of calcium imide into Ca_3N_2 as expected from reaction (1). The structures of calcium nitride hydride (Ca_2NH) and calcium imide (CaNH) are very similar, which results in a similar equivalent lattice parameters. On going from imide to nitride hydride, 50% of the octahedral holes in the closest cubic packing of calcium are now occupied by hydride, rather than nitride/imide ions, with the additional H-sites being vacated, causing a small decrease in the equivalent lattice parameter.

Here we study the structure of calcium nitride hydride (Ca_2NH) using neutron diffraction at temperatures between 20 and 650 °C and correlate structural results with thermal analysis. Breaking up of the N–H ordering would be expected at high temperature and this should have implications on nitrogen and hydrogen mobility within this material's structure. A high mobility of hydrogen is preferable for hydrogen storage purposes as it enhances hydrogen uptake and release. It is thought that this material serves as a good model material to study the mechanisms for hydrogen absorption and desorption processes.

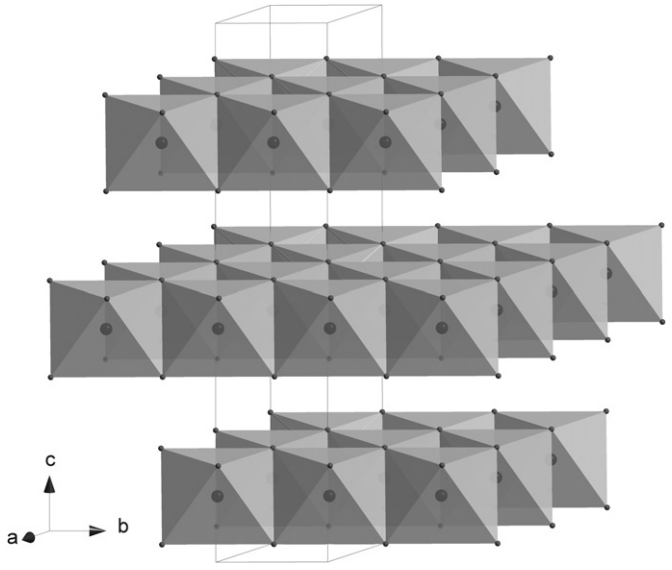

Fig. 1. Structure of Ae_2N with slabs of edge sharing Ae_6N octahedral, separated by empty layers of octahedral holes.

2. Experimental

2.1. Synthesis

Due to the air and moisture sensitive nature of the reactants and products, all handling was carried out in an argon filled glovebox. Ca_2NH was synthesised by combining the elements using the glovebox atmosphere. To this extent, 5% H_2 (BOC, High Purity, 99.995%) and 1–2% N_2 (BOC, 99.998%) had been added to the argon atmosphere in the glovebox. Oxygen and moisture purifiers in the glovebox dry-train minimised oxide and hydroxide contamination during syntheses. Calcium metal (Alfa Aesar, 99.5%) was subsequently fired at 600 °C in a small tube furnace within this glovebox, using an open alumina furnace tube. Molybdenum metal was used as crucible material. $Ca_2ND_{0.90}H_{0.10}$ was prepared in an identical manner, using a 90% deuterium (Spectra Gas, 99.995% chemical purity, 99.7% atom enrichment)/10% hydrogen gas mixture.

Neutron diffraction was carried out on the deuterided sample, $Ca_2ND_{0.90}H_{0.10}$. A mixture of D_2 and H_2 was chosen over either of the pure gases, since the neutron scattering length for H_2 (-3.74 fm) is most dissimilar from that of N_2 (9.36 fm), resulting in significant reflections of ordering peaks, whereas the scattering length for D_2 is 6.67 fm. The large incoherent scattering by H_2 limits its concentration, however, and in order to obtain good data in a reasonable amount of time a 90/10 mixture was chosen. Neutron diffraction data was obtained on diffractometer D1A at ILL, Grenoble, France. The $Ca_2ND_{0.90}H_{0.10}$ powder sample of approximately 1 g was loaded into a vanadium can in a glovebox. A steel cap was fitted on the top of the vanadium can, which prevented the sample from decomposing, whilst transporting the sample to the diffractometer. The neutrons had a wavelength of 1.91 Å (refined to 1.9114 Å). Neutron diffraction patterns were recorded between $0^{\circ}<2\theta<158^{\circ}$ with a resolution of 0.05°, at room temperature (20 °C, RT), 250, 450 and 650 °C, all under vacuum. After heating up to the desired temperature, 20 min was allowed for equilibration.

2.2. Thermal analysis

Thermal analysis results were obtained using a Netzsch STA 449 C Jupiter, which combines differential thermal analysis (DTA) and thermogravimetric analysis (TGA). This setup is linked to a Pfeiffer Vacuum Thermostar mass spectrometer for analysing the gaseous thermal decomposition products. Heating and cooling rates were 5 K/min. Thermal analyses were run in both argon and a mixture of 5% H_2/95% argon.

3. Results

$Ca_2ND_{0.90}H_{0.10}$ was obtained as a yellow powder. CHN elemental analysis reveals a D/H content of 2.04 wt% and an N content of 11.7 wt%, which is in reasonable agreement with the theoretical values of 1.76 wt% (D/H) and 12.7 wt% (N), for a stoichiometric compound. Its neutron powder diffraction pattern is shown in Fig. 2. Indexing of the peaks from the neutron

diffraction data, suggests that the main phase is the nitride hydride/deuteride phase, with $2\times2\times2$ cubic rocksalt type with lattice parameter 10.1550(1) Å in spacegroup *Fd*3*m*, as previously found by Brice et al. [1] and Reckeweg and Di Salvo [13]. Indexing in the rhombohedral spacegroup $R\bar{3}m$, as reported for Ba and Sr nitride hydrides [14,15] is equally successful, with lattice parameters $a=3.58912(1)$ Å and $c=17.600(1)$ Å. A secondary CaO phase was also found, which could be indexed in the *Fm*3*m* spacegroup, with lattice parameter 4.8174(4) Å. This CaO phase most likely results from contamination of calcium during or prior to synthesis. Its phase content was determined to be 20 mol% (12 wt%) from the neutron diffraction refinement and this has been taken into account in all calculations, including CHN and thermal analysis. The diffraction pattern shows no sign of the imide CaNH(D), which reportedly has a slightly larger simple cubic rocksalt lattice parameter of 5.14 Å [16,17]. The lattice parameter obtained using the ordered cubic unit cell for the nitride deuteride phase is in fact slightly but significantly larger than previously found in literature, as shown in Table 1 [1,13,18].

Following indexing, the first refinement in the Fullprof software was carried out using single phase $Ca_2ND_{0.90}H_{0.10}$ (spacegroup *Fd*3*m*, plus secondary phase CaO). The nitride and deuteride ions were placed on 16*d* ($\frac{1}{2}$, $\frac{1}{2}$, $\frac{1}{2}$) and 16*c* (0, 0, 0), respectively, whereas the calcium is positioned slightly off its ideal octahedral site. This is because of a stronger electrostatic attraction of calcium with the nitride ion (N^{3-}) compared to the hydride ion (H^-/D^-) and calcium thus forms distorted octahedra with H(D) and N (as shown in Fig. 3). Considering the colour of the sample (yellow, as opposed to black or dark brown as found by Brice and Sichla), and the CHN results, it is assumed that the compound is stoichiometric (which was also found to be consistent with observed thermogravimetric characteristics), rather than H/D deficient, which would result in a composition $Ca_2NH_{1-\delta}$. Therefore, occupancies for Ca, N and D have been fixed to unity. The resulting crystallographic information from this refinement can be found in Table 2 and it can be seen that the *R*-values are relatively large. This is mainly due to the main diffraction peaks being highly asymmetric, which is most pronounced at higher angle. Also, imperfect matching of peak intensities could be observed.

The strong asymmetry in these peaks at high angle could not be fitted using standard asymmetry functions in the refinement software and instrument D1A is furthermore known to give near Gaussian peak shapes. It was attempted to fit the data using lower symmetry spacegroups, but this did not yield satisfactory results. Furthermore, not all of the peaks exhibit asymmetry and in fact only the reflections for the primitive (non-ordered) cell show this

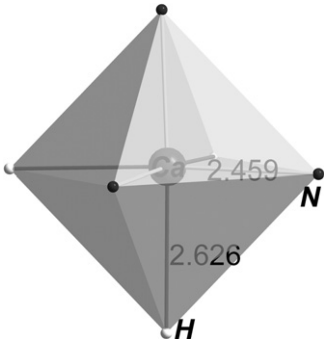

Fig. 3. Distorted CaN_3H_3 octahedron with Ca–N and Ca–H bond lengths.

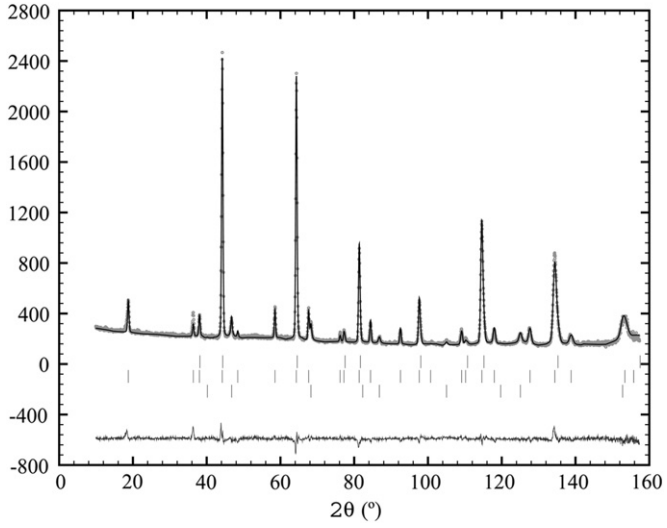

Fig. 2. Neutron powder diffraction pattern of $Ca_2ND_{0.90}H_{0.10}$ at room temperature in grey circles. Refinement shown in black, 3 phases: phase 1 is disordered Ca_2ND, spacegroup *Fm*3*m*, phase 2 is ordered Ca_2ND, spacegroup $R\bar{3}m$, phase 3 is CaO, spacegroup *Fm*3*m*. Ticks show reflections for different phases, bottom grey trail shows residuals after refinement.

Table 2
Refinement of the neutron diffraction pattern for $Ca_2ND_{0.90}H_{0.10}$ at $T=20$ °C, using single phase model for Ca_2ND, spacegroup *Fd*3*m*, and secondary CaO phase (*Fm*3*m*). Neutron wavelength $\lambda=1.91137$ Å.

Refinement parameter	$Ca_2ND_{0.90}H_{0.10}$, *Fd*3*m*		CaO, *Fm*3*m*
a (Å)	10.1551(2)	*a* (Å)	4.8171(4)
V (Å^3)	1047.25(3)	*V* (Å^3)	111.78(2)
Ca, 32e (*x*,*x*,*x*)		Ca, 4*a* (0,0,0)	
x	0.2579(3)	B (Å^2)	1.9(6)
B (Å^2)	1.09(6)		
N, 16*d* ($\frac{1}{2}$,$\frac{1}{2}$,$\frac{1}{2}$)		O, 4*b* ($\frac{1}{2}$,$\frac{1}{2}$,$\frac{1}{2}$)	
B (Å^2)	1.03(4)	B (Å^2)	1.7(5)
D/H, 16*c* (0,0,0)			
B (Å^2)	6.2(1)		
d Ca–N1 (Å)	2.461(3)		
d Ca–D2 (Å)	2.621(3)		
γ N–Ca–N (deg.)	93.67(10)		
γ D–Ca–D (deg.)	86.44(9)		
R_p	4.36		
R_{wp}	5.78		
R_{exp}	2.79		
χ^2	4.29		

Table 1
Comparison of reported structural information on $Ca_2NH(D)$ from literature and data from this work utilising an *Fd*3*m* ordered cell.

Work	Compound	Synthesis temperature (°C)	Product colour	Spacegroup	Lattice parameter (Å)
Brice et al. [1]	Ca_2NH	900–1000	Dark brown	*Fd*3*m*	10.13
Reckeweg and Di Salvo [13]	Ca_2NH	927	Yellow	*Fd*3*m*	10.113
Sichla and Jacobs [18]	Ca_2ND	800	Black	*Fd*3*m*	10.138
This work	$Ca_2ND_{0.90}H_{0.10}$	600	Yellow	*Fd*3*m*	10.1551(2)

behaviour. Therefore this asymmetry cannot simply be attributed to powder morphology of the $Ca_2ND_{0.90}H_{0.10}$ sample either. The best explanation for this asymmetry came from assuming that a second, closely related phase is present. A typical peak at high angle that would arise from the primitive rocksalt, but not its supercell peaks, is illustrated in Fig. 4a. It shows that it slopes towards smaller *d*-spacing and the presence of calcium imide (CaND) with larger cubic lattice parameter can thus be ruled out. Also, from Fig. 2, it can be seen that the asymmetry is not caused by overlapping peaks from the CaO phase. Instead it is assumed that a minor disordered $Ca_2ND_{0.90}H_{0.10}$ phase is present, with slightly smaller lattice parameters. This disordered phase is cubic closest packed in calcium, with N and D(H) each statistically occupying the octahedral sites. It crystallises in spacegroup *Fm*3*m*, with $a_{disordered} \approx (\frac{1}{2}) \cdot a_{ordered}$. This then also explains why the typical ordering peaks of the dominant phase do not show any asymmetry as these are not reflections for the disordered phase (Fig. 4b). Using this 2 phase structural model, the overall quality of the refinement improves significantly, as shown by the improved peak fitting (Fig. 4c) and drop in *R*-values (see Table 3).

The isotropic temperature factor (ITF) for the deuteride ions in the ordered phase is relatively large compared to those for the nitride and calcium ions, *i.e.* 7.3(2) Å^2 for D vs. 1.17(6) Å^2 and 1.16(5) Å^2 for Ca and N, respectively. This might relate to the small content of H in the sample, which will have a larger Ca–H(D) distance in the crystal [19]. Also, although a slightly larger ITF might be expected for the light deuterium, this very large value might indicate some distortion of this site or a lower occupancy of the deuteride site (16*c*). This would be in agreement with Brice et al., who suggested that a fraction of D/H has moved from the octahedral sites to the tetrahedral positions (8*a* site). The refinement in this study improves in fact significantly upon introducing this tetrahedral site. However, only 9% of D/H moves from octahedral to tetrahedral site, which is much less than the 25% found by Brice. As a result, the ITF for D/H is now also slightly lower, *i.e.* 6.3(2) Å^2. The refinement results using

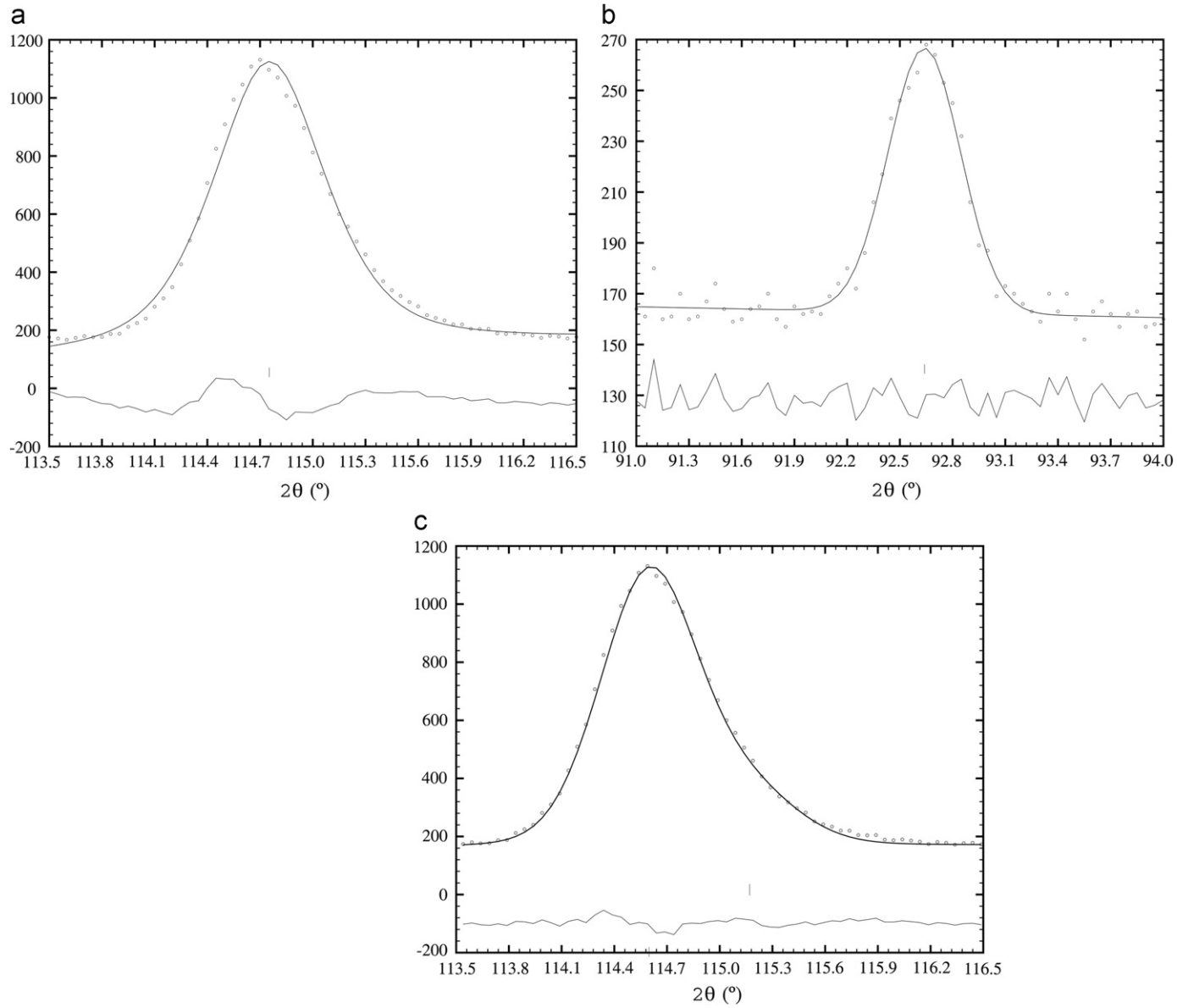

Fig. 4. (a) Peak shape for (840) peak (spacegroup *Fd*3*m*) at high angle and symmetric peak profile fitting (black line), showing bad fit due to asymmetry in data (grey circles), with difference profile below. Note that this peak would be indexed by (420) in the primitive rocksalt cell. (b) Peak shape for typical ordering peak (553)/(731) at high angle, showing proper Gaussian behaviour, note that this peak is not allowed for the primitive rocksalt cell. (c) Improved peak profile fitting (black line) for the (840) peak (spacegroup *Fd*3*m*) shown in Fig. 4a, now using an ordered and a disordered phase.

Table 3
Refinement of neutron diffraction pattern for $Ca_2ND_{0.90}H_{0.10}$, using 2-phase model for Ca_2ND. Phase 1 is disordered, spacegroup *Fm*3*m*; phase 2 is ordered, spacegroup *Fd*3*m* (cubic, N–D ordering in [100] direction). Third phase is CaO (*Fm*3*m*). Neutron wavelength $\lambda = 1.91137$ Å.

	Phase 1: Disordered $Ca_2ND_{0.90}H_{0.10}$ (*Fm*3*m*)		Phase 2: Ordered $Ca_2ND_{0.90}H_{0.10}$ (*Fd*3*m*)
a (Å)	5.0628(4)	*a* (Å)	10.1579(2)
V (Å^3)	129.77(2)	*V* (Å^3)	1048.13(3)
Ca, 4*a* (0,0,0)		Ca, 32*e* (*x*,*x*,*x*)	
B (Å^2)	1.17(6)	*x*	0.2581(2)
		B (Å^2)	1.17(6)
N, 4*b* ($\frac{1}{2},\frac{1}{2},\frac{1}{2}$)		N, 16*d* ($\frac{1}{2},\frac{1}{2},\frac{1}{2}$)	
B (Å^2)	0.2(2)	B (Å^2)	1.16(5)
D/H, 4*b* ($\frac{1}{2},\frac{1}{2},\frac{1}{2}$)		D/H, 16*c* (0,0,0)	
B (Å^2)	0.2(2)	B (Å^2)	7.3(1)
Phase content (mol%)*	8(1)		92(1)
		d Ca–N (Å)	2.460(2)
		d Ca–D (Å)	2.624(2)
		γ N–Ca–N (deg.)	93.76(8)
		γ D–Ca–D (deg.)	86.36(7)
R_p		3.96	
R_{wp}		5.13	
R_{exp}		2.79	
χ^2		3.38	

* Phase content normalised to reflect ratio of ordered vs. disordered. Note that the sample still contains 20 mol% CaO.

this model including a tetrahedral site for D/H can be found in Table 4.

A different ordering mechanism is possible, resulting in N–H ordering in the [111] direction of the cubic unit cell. These structures are generally rhombohedrally distorted and crystallise in the $R\bar{3}m$ spacegroup. The two different types of ordering result in very similar diffraction patterns, which may only be distinguished from a few additional theoretical reflections in the doubled cubic cell, with *Fd*3*m* spacegroup. These additional reflections cannot be observed in our diffraction patterns, however. Although there seems to be no measurable rhombohedral distortion in our $Ca_2ND_{0.90}H_{0.10}$ compound (an ideal ratio of $c/a = 2\sqrt{6}$ is found (see Table 5), which makes the unit cell metrically cubic), we argue that the unit cell with the highest symmetry and smallest volume that fits all the observed peaks, should be chosen as the correct one, which is the cell with spacegroup $R\bar{3}m$ and N–H ordering in the [111] direction. Refining the dominant $Ca_2ND(H)$ phase using a rhombohedral spacegroup also leads to marginally improved *R*-values as evidenced from Tables 4 and 5. As said before, the N–H ordering is more readily explained using the hydrogen intercalation model in the subnitride. The [100] ordering, which has previously been reported for Ca_2NH as the doubled cubic cell is unusual, although it has also been reported for a chemically similar material, Sr_2NF [20]. Indeed, it is conceivable that both types of ordering co-exist within some sort of domain structure but this would be very difficult to refine in a neutron diffraction study. Finally, a fraction of D/H was again allowed to occupy the tetrahedral site (00*z*), with *z* being close to 1/8. For this model with N–H ordering in the [111] direction, 13% D/H is found to transfer from the octahedral site, which is slightly more than was found for the model with N-(D/H) ordering in the [100] direction. Also, the refined *z*-value is in fact significantly lower than 1/8, giving the new *D*/*H* site a

Table 4
Refinement of neutron diffraction pattern for $Ca_2ND_{0.90}H_{0.10}$, using 2-phase model for Ca_2ND. Same as Table 3, however, additional tetrahedral *D*/*H* site included (8*a* site). Neutron wavelength $\lambda = 1.91137$ Å.

	Phase 1: Disordered $Ca_2ND_{0.90}H_{0.10}$ (*Fm*3*m*)		Phase 2: Ordered $Ca_2ND_{0.90}H_{0.10}$ (*Fd*3*m*)
a (Å)	5.0628(4)	*a* (Å)	10.1579(2)
V (Å^3)	129.77(2)	*V* (Å^3)	1048.13(3)
Ca, 4*a* (0,0,0)		Ca, 32*e* (*x*,*x*,*x*)	
B (Å^2)	1.28(5)	*x*	0.2586(2)
		B (Å^2)	1.28(5)
N, 4*b* ($\frac{1}{2},\frac{1}{2},\frac{1}{2}$)		N, 16*d* ($\frac{1}{2},\frac{1}{2},\frac{1}{2}$)	
B (Å^2)	0.5(2)	B (Å^2)	1.22(5)
D/H, 4b ($\frac{1}{2},\frac{1}{2},\frac{1}{2}$)		D1/H1, 16*c* (0,0,0)	
B (Å^2)	0.5(2)	B (Å^2)	6.3(2)
		Occ	0.909(5)
		D2/H2, 8*a* ($\frac{1}{8},\frac{1}{8},\frac{1}{8}$)	
		B (Å^2)	6.3(2)
		Occ	0.182(9)
Phase content (mol%)*	9(1)		91(1)
		d Ca–N (Å)	2.456(2)
		d Ca–D1 (Å)	2.629(2)
		d Ca–D2 (Å)	2.350(2)
		γ N–Ca–N (deg.)	93.98(7)
		γ D1–Ca–D1 (deg.)	86.15(7)
R_p		3.82	
R_{wp}		4.92	
R_{exp}		2.79	
χ^2		3.11	

* Phase content normalised to reflect ratio of ordered vs. disordered. Note that the sample still contains 20 mol% CaO.

triangular coordination with Ca, rather than tetrahedral, as shown in Fig. 5. This could be driven by electrostatic repulsion from N^{3-}, which can be relatively close to the ideal tetrahedral site in this spacegroup. Going from a tetrahedral to a triangular Ca coordination, increases the D2–N distance from 2.20 to 2.50 Å.

It was also attempted to refine the two $Ca_2ND(H)$ phase model to a mixture of rhombohedral and ordered cubic variants, but this yielded poorer fits than the mixture of ordered and disordered variants. This is as expected, as the typical ordering peaks seem to be symmetrical and therefore do not originate from two ordered phases.

Finally, it was attempted to refine cross-substitution of N and D in the rhombohedral phase, to reflect a small degree of disorder. This, however, did not result in better fits and it can therefore be assumed that cross-substitution does not take place at room temperature.

The patterns recorded at 250 and 450 °C could also be refined using this 2-phase model for $Ca_2ND_{0.90}H_{0.10}$, with an ordered and disordered phase. The disordered phase (*Fm*3*m*) content stays constant up to 450 °C, being 8–10(1)%. When the same 2-phase structural model is used for the diffraction pattern obtained at 650 °C, large error estimates in the phase content arise. The evolution of lattice parameters for the two Ca_2ND phases with temperature is shown in Fig. 6. For easy comparison, the rhombohedral lattice parameters have been converted to the equivalent simple cubic lattice parameters. This graph also includes the lattice parameters obtained at 650 °C, when a 2-phase structural model is used. It can be seen that the lattice parameters for the disordered phase are slightly smaller than those obtained for the ordered phase. This can be explained by the

Table 5
Refinement of neutron diffraction pattern for $Ca_2ND_{0.90}H_{0.10}$, using 2-phase model for Ca_2ND. Phase 1 is disordered, spacegroup $Fm\bar{3}m$; phase 2 is ordered, spacegroup $R\bar{3}m$ (rhombohedral, N–D ordering in [1 1 1] direction). Third phase is CaO ($Fm\bar{3}m$). Neutron wavelength $\lambda = 1.91137$ Å.

Refinement parameter	Phase 1: Disordered $Ca_2ND_{0.90}H_{0.10}$ ($Fm\bar{3}m$)		Phase 2: Ordered $Ca_2ND_{0.90}H_{0.10}$ ($R\bar{3}m$)
a (Å)	5.0629(4)	a (Å)	3.5914(2)
		c (Å)	17.594(1)
		$(c/a : 2\sqrt{6})$	1.0000
V (Å^3)	129.78(2)	V (Å^3)	196.52(2)
Ca, 4a (0,0,0)		Ca, 6c (0,0,z)	
B (Å^2)	1.40(6)	z	0.2422(2)
		B (Å^2)	1.40(6)
N, 4b ($\frac{1}{2},\frac{1}{2},\frac{1}{2}$)		N, 3b (0,0,$\frac{1}{2}$)	
B (Å^2)	0.7(2)	B (Å^2)	1.20(4)
D/H,4b ($\frac{1}{2},\frac{1}{2},\frac{1}{2}$)		D1/H1, 3a (0,0,0)	
B (Å^2)	0.7(2)	B (Å^2)	6.1(2)
		Occ	0.867(9)
		D2/H2, 6c (0,0,z)	
		z	0.088(3)
		B (Å^2)	6.1(2)
		Occ	0.067(5)
Phase content (mol%)*	9(1)		91(1)
		d Ca–N (Å)	2.4626(2)
		d Ca–D1 (Å)	2.6213(1)
		d Ca–D2 (Å)	2.074(1)
		γ N–Ca–N (deg.)	93.63(1)
		γ D1-Ca–D1 (deg.)	86.48(1)
R_p		3.80	
R_{wp}		4.91	
R_{exp}		2.79	
χ^2		3.09	

* Phase content normalised to reflect ratio of ordered vs. disordered. Note that the sample still contains 20 mol% CaO.

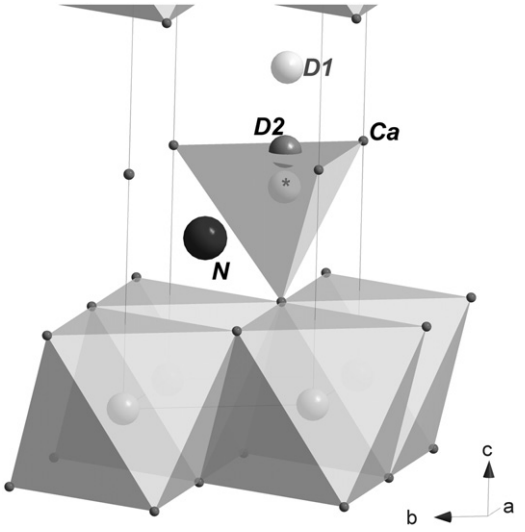

Fig. 5. Part of unit cell, showing DCa_6 octahedrons and an octahedrally coordinated $D1$ site, which may be vacated to be substituted by a triangularly coordinated $D2$ site. Label* marks the ideal tetrahedral site, which probably experiences too much electrostatic repulsion from the nearby N.

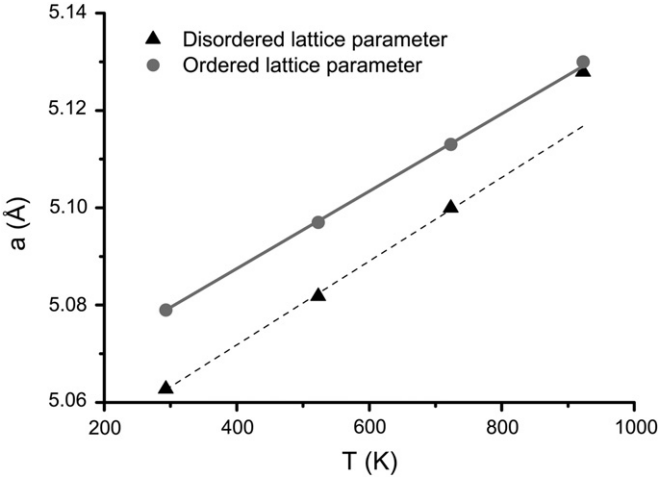

Fig. 6. Lattice parameter of two Ca_2ND phases (disordered and ordered) as a function of temperature. Using the 2-phase model for data set at 650 °C results in near identical equivalent lattice parameter for both phases. Rhombohedral lattice parameters have been converted to equivalent disordered cubic lattice parameter for easy comparison.

absence of distorted CaN_3D_3 octahedra and consequently better packing in the disordered phase. From Fig. 6 it can also readily be seen that at 650 °C, the two phases have identical equivalent lattice parameters. The asymmetry in the peaks at high angle also disappears at 650 °C, suggesting that only a single phase compound remains at this temperature. This in turn explains the large error estimates in phase contents for the 2-phase structural model. Although it would be expected that phases that are unchanged in composition tend to disorder as temperature increase, the neutron diffraction pattern and unit cell size, Figs. 6 and 7 reveal, that it is actually the ordered phase that remains, whereas the disordered phase disappears. The neutron diffraction pattern obtained at 650 °C shows typical ordering peaks, arising from the alternating N and D(H) layers, confirming that ordering remains. The intensity of many of these ordering peaks has, however, decreased significantly, as compared to the patterns obtained at lower temperature. Fig. 7 shows the overlaid diffraction patterns for the same Ca_2ND sample at room temperature and 650 °C. A drastic decrease in relative intensity of the (101) and (021)

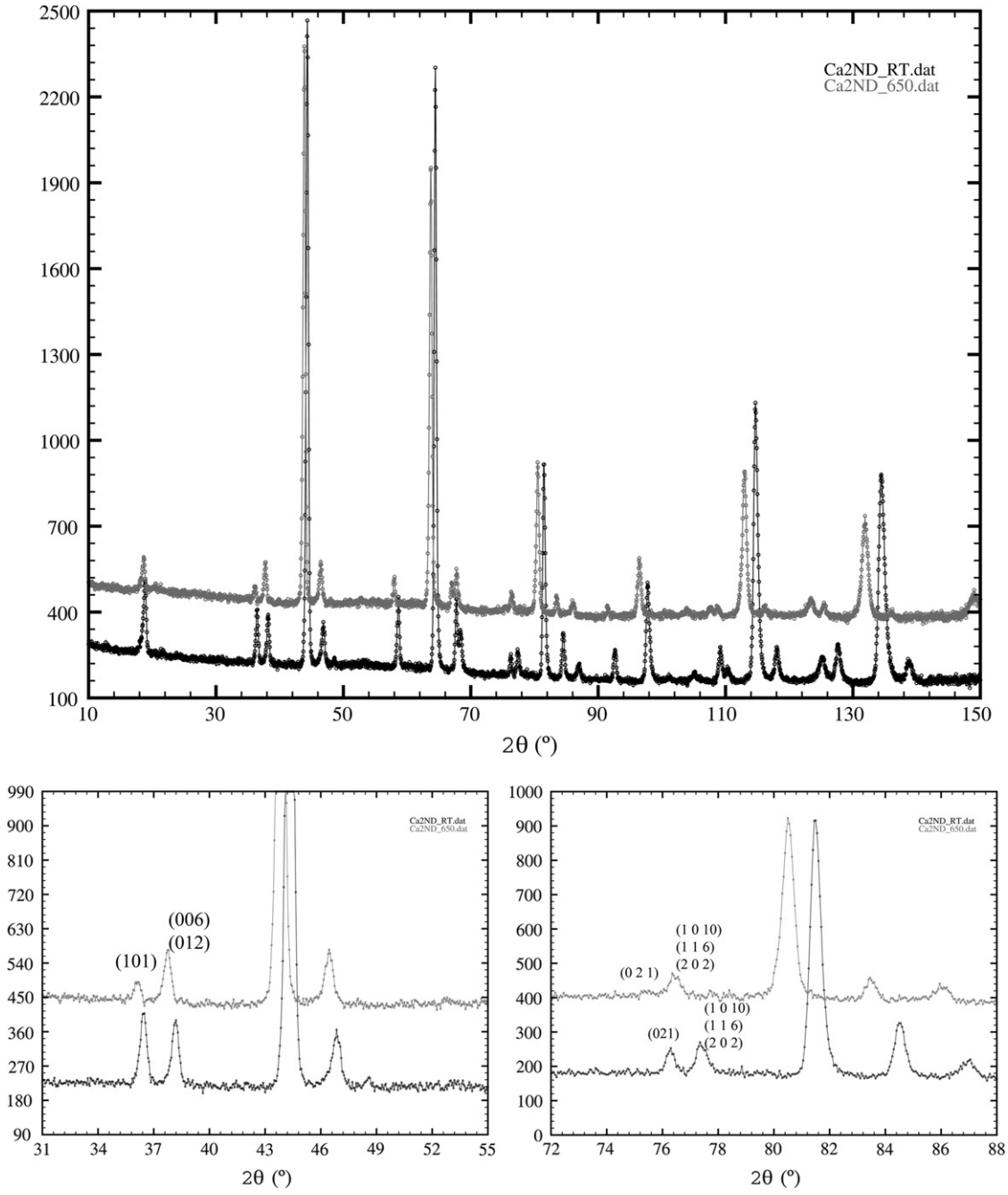

Fig. 7. Neutron powder diffraction patterns for $Ca_2ND_{0.90}H_{0.10}$ at 20 °C (black) and 650 °C (grey), showing a decrease in intensity in peaks typical for ordering, *i.e.* (101) and (021).

peaks that are typical for the ordered rhombohedral lattice, can be seen. It seems therefore that Ca_2ND has gone from a 2-phase *ordered–disordered* material, into a single, partly disordered phase. In such a partly disordered phase, part of the nitride and deuteride ions has swapped between crystallographic sites (between 3*b* and 3*a*, respectively). Before further discussing the unexpected disappearance of the disordered phase at 650 °C, it is important to consider thermal analysis to check for stoichiometry changes.

Fig. 8 shows the thermogravimetric analysis (TGA) for $Ca_2ND_{0.90}H_{0.10}$ in argon atmosphere. Three distinctive events involving a weight loss can be observed. Firstly, a small weight loss occurs at 220–260 °C, which can be explained by the dehydration of surface hydroxides (see reaction (4)), formed during loading of the sample into the thermal analysis equipment. The dehydration temperature is in good agreement with the value of 215 °C reported by Chaix-Pluchery et al. [21], who performed a diffraction study on the dehydration of calcium hydroxide in vacuum. Furthermore, Mass Spectrometry shows that the decomposition products predominantly have ion masses 2, 17 and 18, indicating that water is the main reaction product.

$$Ca(OH)_2 \xrightarrow{T = 220\ ^\circ C} CaO + H_2O \quad (4)$$

The second weight loss occurs at 580–590 °C and involves products with masses 3 and 4, suggesting that gaseous deuterium and HD are released from the Ca_2ND structure. Reckeweg and Di Salvo [13] showed that Ca_2NH could exist with a hydrogen deficiency of up to $\delta = 0.3$ in $Ca_2NH_{1-\delta}$. The weight loss agrees with the

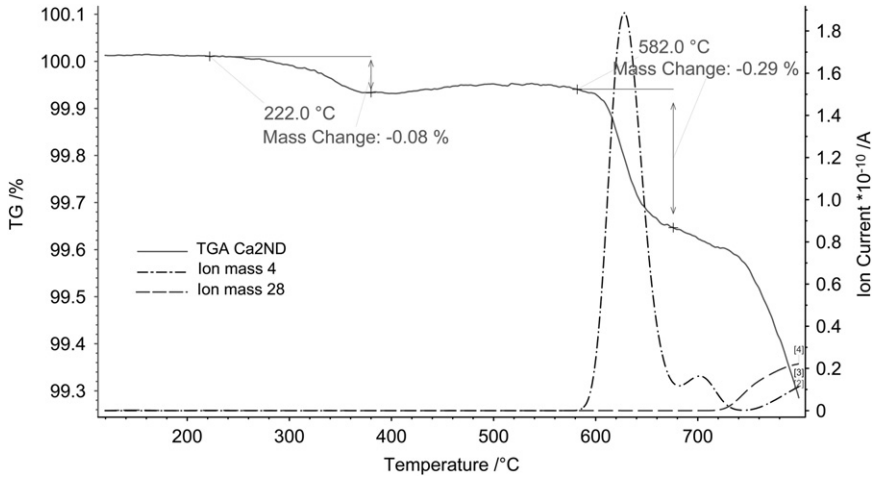

Fig. 8. TGA for $Ca_2ND_{0.90}H_{0.10}$ in argon (solid line). MS ion mass trails, mass 4 (dot–dash) and mass 28 (dash).

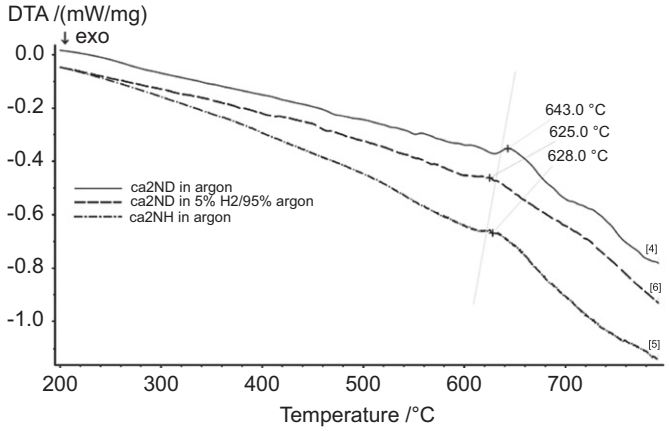

Fig. 9. DTA for $Ca_2ND_{0.90}H_{0.10}$ in argon and 5% H_2/95% argon atmosphere. Also shown is the DTA for Ca_2NH in argon.

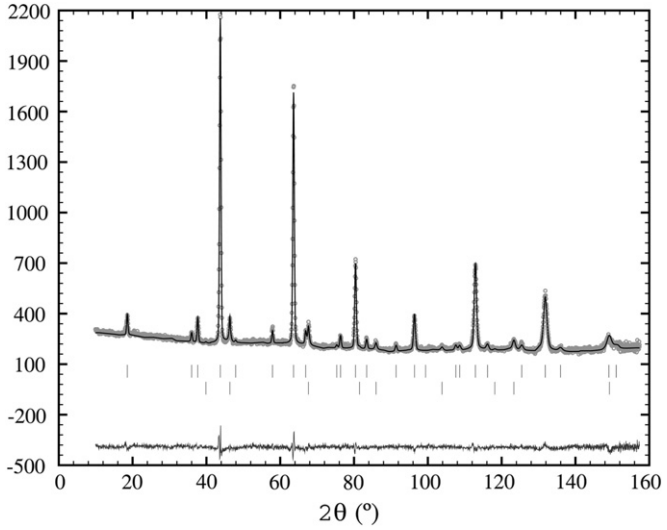

Fig. 10. Neutron powder diffraction pattern of $Ca_2ND_{0.77}H_{0.09}$ at 650 °C in grey circles. Refinement shown in black, 2 phases: phase 1 is partly disordered $Ca_2ND_{0.77}H_{0.09}$, spacegroup $R\bar{3}m$, phase 2 is CaO, spacegroup $Fm3m$. Ticks show reflections for different phases, bottom grey trail shows residuals after refinement.

loss of 0.15 formula units of D/H, so this thermal event is believed to cause a deuterium deficient composition of $Ca_2ND_{0.77}H_{0.09}$. This deuterium content will be used in the neutron diffraction refinement of the pattern recorded at 650 °C. The final weight loss (1.38 wt%, not completely shown in Fig. 8) occurs at 730 °C and involves the release of both nitrogen and deuterium. This final decomposition step does therefore not simply involve the loss of further deuterium to form Ca_2N and the actual decomposition mechanism is not known at the moment. Also, this decomposition step seems to be kinetically hindered; a weight loss of 1.76 wt% is to be expected for Ca_2N as the final product, whereas decomposition into the elements would give a weight loss of 14.6 wt%.

The results from thermogravimetric analysis explain why the disordered component of $Ca_2ND_{0.90}H_{0.10}$ disappears at 650 °C; following D-loss the 2-phase system turns into a single, partly disordered phase. The 2-phase to single phase transition could also be observed in the differential thermal analysis (DTA) of the Ca_2ND sample. Fig. 9 shows the DTA for Ca_2ND in two atmospheres and the DTA for Ca_2NH in argon is also given for comparison. A clear change in the slope can be seen at ~630 °C, indicating the transition from the 2-phase *ordered–disordered* system to the single, partly disordered phase. The small endothermic bump just below this temperature represents the thermogravimetric event of D_2/H_2 loss.

The structural model for the single, partly disordered Ca_2ND phase at 650 °C now also has to include a small understoichiometry for deuterium, as seen from the TGA results. The D/H content was therefore fixed to 0.85. To accommodate a small degree of disorder, nitride and deuteride ions were allowed to cross over between their respective crystallographic sites, *i.e.* 3*b* (0,0,$\frac{1}{2}$) and 3*a* (0,0,0), respectively.

This results in a satisfying fit between refinement and data as shown in Fig. 10. The resulting refinement parameters also seem very reasonable. Firstly, the position of the calcium ion has moved closer to its ideal octahedral site (0,0,$\frac{1}{4}$), as compared to its position at lower temperatures. This is in agreement with the decrease in order and consequently smaller electrostatic effects from the different N and H(D) ions. Secondly, both 3*a* and 3*b* sites total occupancies are about equal, suggesting that the vacancies have been equally spread over both sites. In fact, only nitride ions have moved to the vacant deuteride sites, whereas no deuteride ions occupy nitride sites. During the refinement process, it was also noticed that the additional triangular site for D/H has practically disappeared (in fact the site has moved so far away from triangular coordination, making it practically identical to the octahedral *D*/*H* site). The thermal event leading to the formation

Table 6
Refinement results for $Ca_2ND_{0.90}H_{0.10}$ at 650 °C. Single, partly disordered phase, spacegroup $R\bar{3}$ m, involving N^{3-} and D^{-} crossing over between their respective crystallographic site. Neutron wavelength λ=1.91,137 Å.

Refinement parameter	
a (Å)	3.62,633(1)
c (Å)	17.767(1)
V (Å^3)	202.33(1)
Ca, 6c (0,0,z)	
x	0.2444(3)
B (Å^2)	3.15(6)
N1, 3b (0,0,$\frac{1}{2}$)	
B (Å^2)	2.30(5)
Occ	0.91(1)
D1/H1, 3b (0,0,$\frac{1}{2}$)	
B (Å^2)	2.30(5)
Occ	0.00(1)
D2/H2, 3a (0,0,0)	
B (Å^2)	5.2(1)
Occ	0.85(1)
N2, 3a (0,0,0)	
B (Å^2)	5.2(1)
Occ	0.09(1)
d Ca–N (Å)	2.508(3)
d Ca–D (Å)	2.623(3)
γ N–Ca–N (deg.)	92.59(9)
γ D–Ca–D (deg.)	87.46(10)
R_p	3.19
R_{wp}	3.81
R_{exp}	2.75
χ^2	1.92

of $Ca_2ND_{0.77}H_{0.09}$ can therefore now be related to the loss of D/H from the interstitial triangular sites. The loss of 0.15 formula units D/H found in thermal analysis, matches up well with the initially 6.7% occupied triangular sites (*i.e.* 0.13 formula units). The refinement results have been summarised in Table 6.

4. Discussion and conclusions

$Ca_2ND_{0.90}H_{0.10}$ was synthesised from the elements at 600 °C. A 2-phase system resulted, consisting of closely related disordered and ordered Ca_2ND phases. The ordered phase is best described using a rhombohedral spacegroup $R\bar{3}m$, resulting in closest packed layers of Ca and alternating layers of nitride and deuteride ions. This model is different from that reported previously by Brice et al. [1] and Sichla et al. [18]. In those studies, a doubled cubic cell with spacegroup $Fd\bar{3}m$ was used to represent the N–H ordering in this compound. Whereas in the current study a geometrically cubic compound is also found, all reflections in the neutron diffraction pattern could be indexed using a smaller unit cell, with rhombohedral spacegroup $R\bar{3}m$. Using a doubled cubic cell would lead to additional reflections, none of which could be observed in our experiments. The resulting N–H ordering for this $R\bar{3}m$ spacegroup also seems more reasonable when nitride hydride compounds are considered to be subnitrides (Ae_2N) intercalated with hydride ions. Furthermore, the current model is in agreement with the existing models for Sr_2NH and Ba_2NH [14,15]. These two compounds are in fact significantly rhombohedrally distorted. Upon heating to 650 °C, the disordered phase content decreases due to a deuterium/hydrogen loss at 580 °C and a single phase compound remains. This high temperature single $Ca_2ND_{0.77}H_{0.09}$ phase is best described as a partially disordered material, in which some of the N and D swap crystallographic sites. The observed deuterium loss is furthermore believed to be caused by the disappearance of an interstitial triangular site, which at lower temperatures accommodates 13% of structural D/H.

Supporting information available

Refinement information for neutron powder diffraction data at 20, 250, 450 and 650 °C in Crystallographic Information File (CIF).

Acknowledgments

The authors would like to thank EPSRC for funding.

Appendix A. Supplementary material

Supplementary data associated with this article can be found in the online version at doi:10.1016/j.jssc.2011.05.062.

References

[1] J.F. Brice, J.P. Motte, A. Courtois, J. Protas, J. Aubry, Journal of Solid State Chemistry 17 (1–2) (1976) 135–142.
[2] P. Chen, Z.T. Xiong, J.Z. Luo, J.Y. Lin, K.L. Tan, Nature 420 (6913) (2002) 302–304.
[3] W.F. Luo, Journal of Alloys and Compounds 381 (1–2) (2004) 284–287.
[4] Z.T. Xiong, P. Chen, G.T. Wu, J.Y. Lin, K.L. Tan, Journal of Materials Chemistry 13 (7) (2003) 1676–1680.
[5] Y.F. Liu, T. Liu, Z.T. Xiong, J.J. Hu, G.T. Wu, P. Chen, A.T.S. Wee, P. Yang, K. Murata, K. Sakata, European Journal of Inorganic Chemistry 21 (2006) 4368–4373.
[6] Y.F. Liu, Z.T. Xiong, J.J. Hu, G.T. Wu, P. Chen, K. Murata, K. Sakata, Journal of Power Sources 159 (1) (2006) 135–138.
[7] G.T. Wu, Z.T. Xiong, T. Liu, Y.F. Liu, J.J. Hu, P. Chen, Y.P. Feng, A.T.S. Wee, Inorganic Chemistry 46 (2) (2007) 517–521.
[8] Z.T. Xiong, G.T. Wu, H.J. Hu, P. Chen, Advanced Materials 16 (17) (2004) 1522–1525.
[9] H. Wu, Journal of the American Chemical Society 130 (20) (2008) 6515–6522.
[10] D.H. Gregory, Journal of Materials Chemistry 18 (20) (2008) 2321–2330.
[11] R. v. Juza, H. Schumacher, Zeitschrift für anorganische und allgemeine Chemie 324 (1963) 278–286.
[12] J. Senker, H. Jacobs, M. Muller, W. Press, P. Muller, H.M. Mayer, R.M. Ibberson, Journal of Physical Chemistry B 102 (6) (1998) 931–940.
[13] O. Reckeweg, F.J. DiSalvo, Solid State Sciences 4 (5) (2002) 575–584.
[14] R. Chemnitzer, G. Auffermann, D.M. Tobbens, R. Kniep, Zeitschrift Für Anorganische Und Allgemeine Chemie 631 (10) (2005) 1813–1817.
[15] B. Wegner, R. Essmann, J. Bock, H. Jacobs, P. Fischer, European Journal of Solid State and Inorganic Chemistry 29 (6) (1992) 1217–1227.
[16] T. Sichla, H. Jacobs, Zeitschrift Für Anorganische Und Allgemeine Chemie 622 (12) (1996) 2079–2082.
[17] H. v. Hartmann, H.J. Fröhlich, F. Ebert, Zeitschrift für anorganische und allgemeine Chemie 218 (1934) 181–189.
[18] T. Sichla, H. Jacobs, European Journal of Solid State and Inorganic Chemistry 32 (1) (1995) 49–56.
[19] A.R. Ubbelohde, Transactions of the Faraday Society 32 (1936) 525–529.
[20] T.R. Wagner, Journal of Solid State Chemistry 169 (1) (2002) 13–18.
[21] O. Chaix-Pluchery, J. Bouillot, D. Ciosmak, J.C. Niepce, F. Freund, Journal of Solid State Chemistry 50 (2) (1983) 247–255.